



The cerebellum coordinates eye and hand tracking movements

R. C. Miall¹, G. Z. Reckess² and H. Imamizu³

¹ University Laboratory of Physiology, Parks Road, Oxford, OX1 3PT, UK

² Department of Experimental Psychology, South Parks Road, Oxford, OX1 3UD, UK

³ Kawato Dynamic Brain Project, ERATO, JST, 2-2 Hikaridai, Seika, Soraku, Kyoto 619-0288, Japan

Correspondence should be addressed to R.C.M. (chris.miall@physiol.ox.ac.uk)

The cerebellum is thought to help coordinate movement. We tested this using functional magnetic resonance imaging (fMRI) of the human brain during visually guided tracking tasks requiring varying degrees of eye–hand coordination. The cerebellum was more active during independent rather than coordinated eye and hand tracking. However, in three further tasks, we also found parametric increases in cerebellar blood oxygenation signal (BOLD) as eye–hand coordination increased. Thus, the cerebellar BOLD signal has a non-monotonic relationship to tracking performance, with high activity during both coordinated and independent conditions. These data provide the most direct evidence from functional imaging that the cerebellum supports motor coordination. Its activity is consistent with roles in coordinating and learning to coordinate eye and hand movement.

The cerebellum is thought to be an important neural component in coordination¹ among the joints of one limb^{2,3}, between two limbs⁴, between the eye and hand in reaching, pointing or tracking tasks^{5–8}, or between the eye and leg during gait⁹. Here we address the cerebellum's contribution to coordination between the eye and hand in a visually guided tracking task. We operationally define coordination as the process facilitating motor performance during synchronous, spatially coherent movement of two effectors. Thus, coordination is found when rubbing one's own head and stomach with both hands—the two hands move at the same rate, in symmetric directions, and in synchrony, although they are spatially separated. In contrast, trying to rub with one hand and tap with the other is much more difficult because independent control of the two hands is required.

We used a tracking task in which subjects followed a moving target with their eyes while simultaneously moving a joystick to control a cursor. This protocol allows parametric variation of the degree of coordination between eyes and hand. The target trajectories followed by eye and hand may be identical, allowing maximal cooperation between the two control systems; they may be completely independent, causing interference between the two, or with graded levels of correspondence by temporal offset between their respective trajectories (Fig. 1). We first used fMRI to detect those brain sites activated by eye and hand movement performed alone or together, and in a second experiment found regions whose activity parametrically co-varied with the degree of coordination between ocular and manual tracking movements. Additional experiments confirmed the non-monotonic relationship between performance and cerebellar activation suggested by the first two experiments.

RESULTS

We monitored joystick movement throughout each task condition (Fig. 1). Manual joystick tracking was significantly better when the target trajectories for eye and hand were identical and

synchronous ('coordinated condition') than when they were unrelated ('independent condition') with 20% reduction in root mean squared (RMS) error and 37% reduction in tracking lag ($p < 0.001$, matched pairs t -tests). Performance when tracking with the hand alone ('hand only') was worse than in the coordinated eye and hand condition (17% increase in lag, $p = 0.03$; 3% increase in RMS error, not significant), but better than in the independent condition (RMS error and lag, $p < 0.001$). These differences were confirmed in laboratory conditions in an independent group of seven subjects tested in greater detail (R.C.M. & G.Z.R., *Eur. J. Neurosci.* **12 Suppl.** **11**, 40.11, 2000; R.C.M. & G.Z.R., unpublished data). Hence, as expected from existing literature^{10–13}, coordinated eye–hand tracking conferred a significant advantage over independent but synchronous eye–hand control and over manual tracking alone.

Manual tracking performance recorded in the MR scanner was not significantly different from that recorded from seven subjects tested in detail in the laboratory (Fig. 2). RMS errors and mean lag rose with increasing temporal offset, whereas optimal performance was achieved for the scanned group when the target for eye motion anticipated that for hand motion by some 38 ms (estimated by second-order polynomial interpolation of the heavy curves in Fig. 2). Differences in RMS errors were not significant in this group, but mean lag did vary significantly with temporal offset ($F_{4,40} = 2.86$, $p < 0.04$, ANOVA). For subjects tested in the laboratory, both error and mean lag varied highly significantly ($F_{13,273} > 4.5$, $p < 0.0001$, ANOVA), and minimum RMS error was estimated to be at an offset of 61 ms. These data support our view that the temporal asynchrony of target trajectories provided a parametric manipulation of eye–hand coordination, and also show that optimal performance was achieved when the ocular system slightly anticipated the manual system.

Ocular tracking could not be recorded in the MR scanner and is not considered here in detail (R.C.M. & G.Z.R., unpublished data). However, we recorded eye position during these

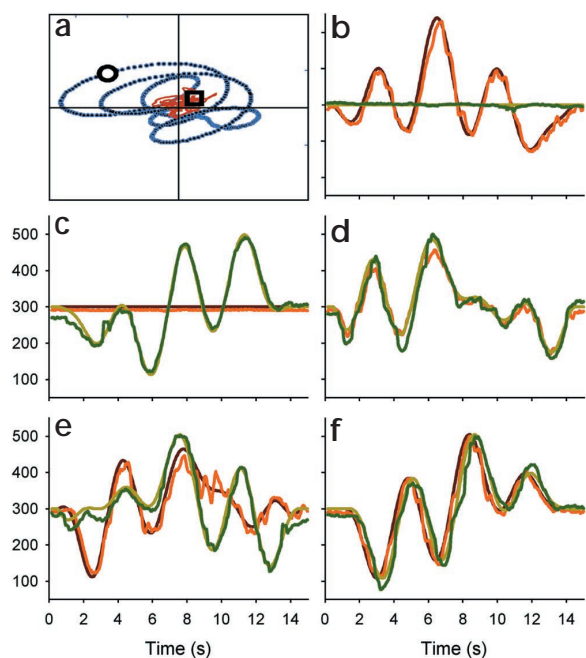


Fig. 1. Tracking task. (a) Subjects tracked a displayed moving circle (blue trajectory) with eye movement. They also used a joystick to correct for target motion of a square cursor away from a central crosshair. Red, on-screen cursor trajectory. Accurate tracking in the coordinated condition led to movement of the joystick along the same trajectory as the eyes. (b–e) Four factorial conditions: hand only (b), eye only (c), coordinated (d) and independent (e). For clarity, only horizontal components of the trajectories are shown. Target trajectories for the hand (dark red) and for the eye (yellow) are the smooth lines; the trajectories of the joystick (orange) and the eye (green) are more jerky. (f) An example of the -304 ms temporal offset condition of experiment 2, with manual target trajectory leading the ocular trajectory.

tasks in another group of six subjects, whose manual tracking performance confirmed the significant results listed above for both experiments 1 and 2. Eye tracking performance did not vary significantly with condition in either experiment (correlation to ocular target, correlation and lag, $p > 0.05$, ANOVA,

Table 1. Location of clusters of significant activation during manual tracking and ocular tracking, factorial experiment 1.

(a) Ocular tracking versus rest						
Cluster size (cc)	Cluster p ($n_{\max} \geq k$)	Max Z score	Peak x mm	Peak y mm	Peak z mm	Location
77.34	< 0.00001	9.3	-18.8	-48.7	59.0	L PPC/SM BA 7/2
12.38	< 0.00001	7.9	-45.5	-66.5	11.0	L MT/V5 BA 19
10.16	< 0.00001	7.0	-30.7	-4.1	47.0	L PM BA 6
8.67	< 0.00001	11.2	46.5	-66.5	11.0	R MT/V5 BA 19
3.59	0.00014	4.5	-1.0	-78.4	-37.0	Cerebellar vermis (VIII)
(b) Manual tracking versus rest						
29.30	< 0.00001	6.2	-30.7	-33.8	53.0	L SMC BA 2/4
13.17	< 0.00001	6.1	-36.6	-72.5	11.0	L PPC BA 39
9.84	< 0.00001	4.8	34.6	-39.8	53.0	R SMC BA 2
9.20	< 0.00001	5.7	40.5	-63.6	5.0	R extrastriate BA19
9.05	< 0.00001	4.8	25.7	1.8	5.0	R BG putamen
5.24	< 0.00001	5.3	-16.8	-16.0	-7.0	L BG pallidum
4.28	0.00005	4.6	-57.3	-13.0	41.0	L SMC BA 2/4
2.33	0.00827	5.16	31.2	-84.3	-13.0	R cerebellum (crus I)

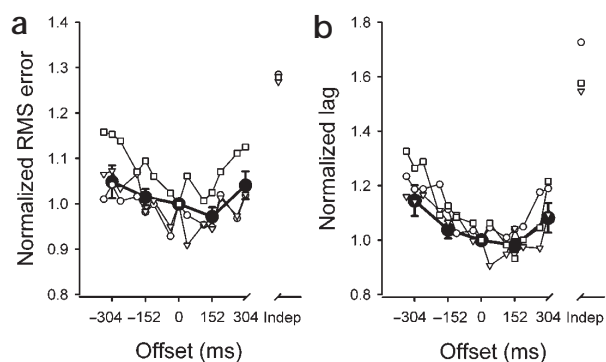


Fig. 2. Effect of eye–hand temporal offset on manual tracking performance. Positive offset values indicate that the target for eye movement anticipated that for hand movement; negative values indicate the reverse. (a) Mean RMS errors normalized to the synchronous condition. Heavy line, mean performance data (± 1 s.e.m.) from the MR scanning sessions of experiment 2 ($n = 9$). Fine lines, mean data from another 7 subjects tested at target speeds 35% slower (triangle), same (circle) or 35% faster (square) than used in the fMRI experiment; independent eye–hand data is at the far right. (b) Mean tracking lag, estimated from cross-correlation of joystick and manual target trajectories.

$n = 6$). Examination of all 360 records confirmed that the subjects were able to follow the ocular target at almost all times. The total time spent in blinks, in brief (0.2–0.5 s) fixation of the manual target (for example, Fig. 1c, at 4 s) or in very occasional mistaken pursuit of the cursor ranged across subjects from 0.2–1.5% of the task duration.

Coordinated versus independent eye–hand control

Contrasting ocular tracking versus fixation activated areas in extrastriate visual cortex, parietal cortex and cerebellar vermis, consistent with ocular tracking of a moving target (Table 1a)^{14–16}. The cortical eye fields may not be activated because the baseline task was ocular fixation. Contrasting manual tracking ('hand only,' Table 1b) versus rest activated the areas expected^{16–18} to be involved in control of right hand motion within contralateral sensory–motor and premotor areas, and bilateral areas in basal ganglia and ipsilateral cerebellum. Interaction terms of the factorial analysis (see Methods) exposed regions significantly more active in the coordinated condition than expected by summation of their activity in ocular and hand-only conditions (that is (coordinated + rest) – (hand only + eye only)), with activation of precuneus, extrastriate visual cortex, and weaker activation of prefrontal and ventral premotor regions (Table 2a). Bilateral lateral cerebellum was also activated, replicating an earlier fMRI tracking experiment⁸.

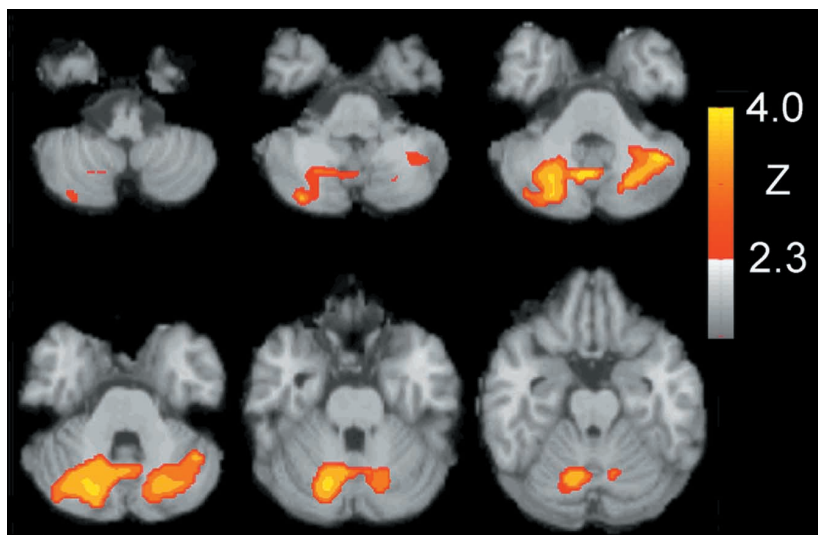
Directly contrasting activity during coordinated and independent conditions again resulted in significant bilateral activation of precuneus, right ventral premotor cortex, left superior and inferior parietal cortex, and right basal ganglia (Table 2b); however, this contrast did not activate cerebellum. Conversely, contrast of independent against coordinated tracking significantly activated only the medial cerebellum with peaks within the cerebellar nuclei (Table 2c).

Parametric variation of eye–hand coordination

There were highly significant performance differences between the coordinated and independent conditions



Fig. 3. Parametric analysis of BOLD related to eye–hand temporal offset. Significant activity in experiment 2 was constrained entirely to the cerebellum (cluster, $p = 0.0006$, random effects group analysis, $n = 9$). Axial slices are at 5 mm separation from -46 mm relative to the AC-PC line⁴⁸. The right brain is on the left of each image.



of experiment one, whereas the enforced eye–hand asynchrony in experiment two introduced smaller, graded performance changes within the same general tracking task. We therefore tested for BOLD activation in the second experiment fitted by quadratic regression to the temporal offset parameter. A positive relationship would expose areas that co-varied with the U-shaped RMS error and tracking lag performance curves (Fig. 2). No areas were found to be activated at normal statistical significance levels for this positive model ($p > 0.01$, fixed-effects group analysis). Conversely, a negative relationship would expose areas that were maximally active when performance was good and less active when performance was degraded by the eye–hand asynchrony. This model resulted in a large activation pattern within the cerebellum, statistically significant with both fixed-effects and the more conservative random-effects group analyses (Fig. 3). Peak activation loci were in the bilateral dentate nuclei, in the adjacent cerebellar cortex: crus

1, lobules VI and VII, and the oculomotor vermis (Table 3). No significant activity was seen in any other brain area.

The relationship between performance and BOLD

The factorial design of experiment 1 demonstrated that the cerebellum was more activated during the independent condition, when performance errors were high, than in the coordinated condition. The parametric design of experiment 2 showed that it was more activated during the coordinated condition, when performance errors were low, than in the temporal offset conditions. These results imply a non-monotonic relationship between performance error and BOLD signal within the cerebellum.

We tested this prediction with additional combined experiments in which subjects were tested in the same session with the coordinated condition (zero offset), different temporal offset conditions, and the independent condition used in experiment 1. BOLD signal was fitted by weighted regression to these task parameters as before. In experiment 3, our regression model assumed the same inverted-U function as used in experiment 2, combined with a high positive weighting for the independent condition (see Methods). Significant bilateral cerebellar activity was found (Fig. 4, Table 4) with clear overlap in activation patterns between experiment 2 and 3. In experiment 4, we tested for a dip in BOLD signal within the monotonically increasing performance curves (Fig. 5a and b). The signal from the cerebellum was significantly fitted by the quadratic U-shaped model (Table 5a). No areas were significantly activated by an inverted-U model ($p > 0.01$, fixed-effects group analysis). As predicted, both contrasts of the coordinated (zero offset) and the independent condition with the -304 ms condition resulted in significant cerebellar activation (Fig. 4c, Table 5b and c). There was about 50% overlap of the activation patterns within the cerebellum, in crus I and lobules VII and VIII. Contrast between the coordinated and independent conditions confirmed the activation of

Table 2. Significant clusters and local maxima from factorial analysis of experiment 1.

(a) Coordination versus isolated movement: positive interaction terms						
Cluster size (cc)	Cluster p ($n_{\max} \geq k$)	Max Z score	Peak x mm	Peak y mm	Peak z mm	Location
51.47	< 0.00001	5.32	-4.0	-39.8	35.0	Bilateral precuneus BA 7/31
10.84	< 0.00001	4.33	25.7	-72.5	-1.0	R extrastriate BA 18
		3.87	16.8	60.6	-7.0	R lateral cerebellum (VI/IV)
9.57	0.00017	3.81	18.8	37.5	35.0	R prefrontal BA 32
5.45	< 0.00001	4.21	-21.8	-42.8	-13.0	L lateral cerebellum (V)
5.34	0.00021	3.37	49.4	1.1	17.0	R PMV/insula
3.44	0.00630	3.53	-45.5	4.1	17.0	L PMV/insula
(b) Coordinated versus independent tracking						
15.39	< 0.00001	4.03	10.9	-54.6	23.0	Bilateral precuneus BA 7/31
		3.71	-36.6	-63.6	23.0	L PPC BA 39
7.93	0.00017	4.31	22.7	-7.1	-7.0	R BG pallidum
		3.62	34.6	7.8	-13.0	R PMV/insula
(c) Independent versus coordinated tracking						
8.73	0.00007	3.53	10.7	-60.6	-31.0	R cerebellum (interposed n.)
		3.49	9.9	57.6	-31.0	L cerebellum (interposed n.)

Table 3. Significant local maxima (random effects group analysis) from parametric analysis of experiment 2.

Cluster size (cc)	Cluster p ($n_{\max} \geq k$)	Max Z score	Peak x mm	Peak y mm	Peak z mm	Location
22.96	0.00060	3.856	4.9	-63.6	-37.0	R posterior vermis (lobule VIII)
		3.777	-39.5	-51.7	-37.0	L lateral posterior lobe (VII, crus I)
		3.561	16.8	-69.5	-25.0	R posterior lobe (VI, declive)
		3.400	28.7	-75.5	-37.0	R posterior lobe (VII, crus I)
		3.356	28.7	-63.6	-37.0	R dentate n.
		3.026	-24.7	-63.6	-37.0	L dentate n.

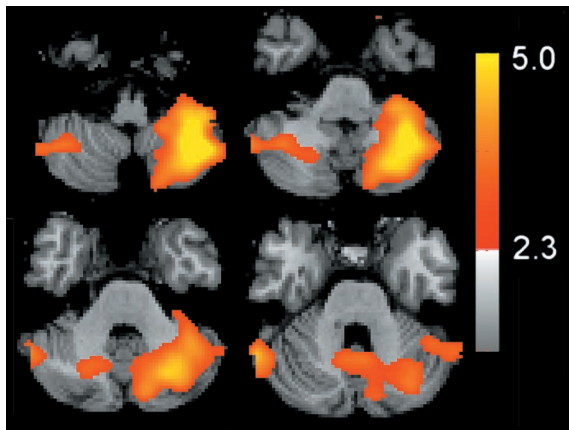


Fig. 4. Combined independent and temporal offset conditions. Significant activity is shown that was modeled by both independent tracking and eye–hand temporal offset parameters. The right brain is on the left of each image; axial slices are at -48 , -42 , -36 and -30 mm relative to AC–PC. (Data from experiment 3, fixed effects, $n = 7$).

precuneus seen in the factorial experiment (Table 5d). No significant activity was seen for the reverse contrast.

DISCUSSION

We show that the cerebellum was significantly activated in coordinated eye–hand tracking compared to isolated eye and hand movements, and that the cerebellum and only the cerebellum varied its activity in parametric relationship with the temporal offset used to vary eye–hand coordination. We confirmed these results in additional combined experiments, exposing a non-monotonic relationship between tracking error and cerebellar BOLD signal.

Functional imaging cannot be used to claim causal relationships. However, the improvement in tracking performance that we observed when eye–hand tracking was nearly synchronous must result from involvement of an active coordinating process, because coordinated eye–hand tracking was better than movement of the hand alone. Hence, these results argue strongly that cerebellar activity underlies the good performance in the eye–hand coordinated conditions of our task.

The lack of cerebellar activity in the direct contrast of coordinated versus independent conditions in the first factorial experiment was initially puzzling. Confirmation of this result in two combined parametric experiments (3 and 4) showed that the cerebellum was more heavily activated in the independent task, during correction of and learning from the significant movement errors^{20–23}. Significant activity was indeed found in the contrast between the independent condition—when tracking errors were 20% higher—and coordinated condition (experiment 1, Table 2c; experiments 3 and 4). Similar activity was seen in the contrast of the independent condition with the -304 ms condition (experiment 3 and 4; Fig. 5c). This activation might also be related to factors other than movement error, as the independent task probably required higher attentional levels²⁴ and involved more independent stimulus–response mapping²⁵, but these were not independently manipulated here.

Table 4. Significant cerebellar local maxima (fixed effects group analysis, $n = 7$) from experiment 3; combined response to asynchrony and independence.

Cluster p ($n_{\max} \geq k$)	Max Z score	Peak x mm	Peak y mm	Peak z mm	Location
<0.00001	5.76	-40	-54	-38	Left, posterior lobe (crus II)
	4.37	62	-56	-24	Right, posterior lobe (crus I)
	4.03	-22	-42	-54	Left, dentate n.
	3.57	-12	-74	-36	Left, posterior lobe (crus I)
	3.36	42	-52	-44	Right, posterior lobe (lobule VII/VIII)
	3.08	-2	-56	-30	Posterior vermis (lobule VIII)
	3.00	30	-56	-38	Right, dentate n.

However, cerebellar activity was not simply related to conditions with high movement errors. We found significant and robust cerebellar activation in the coordinated condition of each parametric experiment (2, 3 and 4; Figs. 3, 4 and 5), exposing a positive relationship between improved performance and BOLD signal. Thus, large tracking errors seem to induce measurable activity within the cerebellum that can hide smaller activity changes related to coordination. In motor learning tasks^{20–23}, high cerebellar activity related to performance errors is typically seen early on. Weaker cerebellar activation sustained after the motor learning is also seen^{20,22,26}. The activity patterns we saw (Tables 2c, 4 and 5; Figs. 3, 4 and 5) are consistent with this.

It is also striking that the precuneus was significantly more active in the coordinated condition than in either the independent eye–hand condition (experiments 1, 3 and 4) or the hand-only conditions (experiment 1). The precuneus has not been reported to be involved in coordination but is active in visual imagery, visual–spatial processing and navigation^{17,27–29}, and attentive tracking³⁰. Our coordinated tracking task gives the subject opportunities to visualize the required manual trajectories from visual cues and from extraretinal signals³¹. Thus, activation of the precuneus

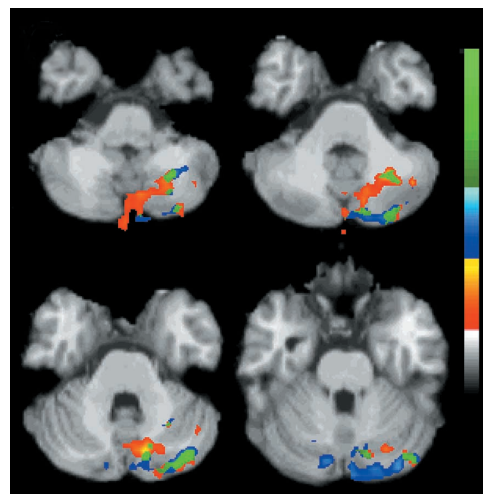
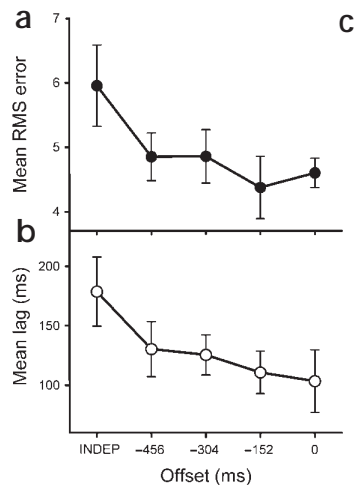


Fig. 5. Testing for non-monotonic BOLD signal. RMS manual tracking error (a) or tracking lag (b) against the five conditions of experiment 4. (c) Areas of significant cerebellar activation for the contrast of independent versus -304 ms offset (red), coordinated versus -304 ms (blue) and their overlap (green). Axial slices are at -41 , -36 , -31 and -26 mm relative to AC–PC.

**Table 5. Significant local maxima (fixed-effects group analysis, $n = 3$) from experiment 4.**

Cluster size (cc)	Cluster p ($n_{\max} \geq k$)	Max Z score	Peak x mm	Peak y mm	Peak z mm	Location
(a) Combined response to asynchrony & independence						
25.03	<0.00001	4.86	14.0	-68.0	64.0	PPC BA 7
12.53	0.00001	3.92	-30.0	-58.0	-36.0	L cerebellum, dentate n.
(b) Coordinated versus -304 ms asynchronous tracking						
14.12	0.00002	3.90	-34.0	-80.0	-28.0	L cerebellum (crus I)
14.10	0.00002	4.20	14.0	-68.0	64.0	PPC BA 7
(c) Independent versus -304 ms asynchronous tracking						
16.80	<0.00001	4.26	-34.0	-72.0	-52.0	L cerebellum (VII, VIII)
11.22	0.00017	3.85	-26.0	-56.0	74.0	L PPC BA7
9.91	0.00050	3.96	44.0	46.0	8.0	R prefrontal/insula BA 45/46
(d) Coordinated versus independent tracking						
5.42	0.00840	3.26	-2.0	-44.0	36.0	Bilateral precuneus/BA 7/31

is unlikely to be directly related to coordination, but instead to integration of these visuo-spatial cues into selection and planning of hand movements³².

Motor coordination depends on predictive information about movement. Synchronous movement of two effectors cannot be achieved simply by reaction to reafferent proprioceptive or visual inputs^{12,33,34}. In our factorial experiment, coordinated tracking was more accurate than tracking with hand movement alone. Hence, a predictive 'forward model' estimate³⁵ of the movement outcome based on motor commands being sent to one effector^{36,37} is probably used to program or modify the movement of the other effectors. We believe that Figs. 3 and 4 reveal the activation of these internal models, exposed by their sensitivity to the eye-hand temporal asynchrony. Asynchrony ranging from ± 304 ms caused greatest changes in the mean tracking lag (Figs. 2b and 5b), with smaller changes in RMS error and only small changes in peak correlation coefficients. However, the mean change in tracking lag across these conditions was under 30 ms: subjects were not simply reproducing hand movements that were time-locked to their eye movements. Thus, our experimental manipulation disrupted performance by causing temporal mismatches in the forward predictions of eye and hand movement, and consequently, performance suffered. Similar performance deficits can also be seen if sensory feedback is delayed^{34,38,39} because of the temporal mismatch between predicted and actual movement outcome.

Finally, we address a question of functional imaging interpretation common to motor coordination and to learning. If the cerebellum is the neural center for coordination, we might expect it to try to coordinate eye-hand movements under all circumstances, even if it fails in some. Why, then, do neural responses and BOLD signals change across our conditions? Recent theory⁴⁰ suggests that the cerebellar learning process may include active selection of control modules based on the goodness of fit of their forward modeling of current sensory-motor conditions. We suppose that the active models contribute to the BOLD signal in the coordinated condition. However, in the unusual circumstance when eye-hand asynchrony was enforced, modules that normally predict synchronous eye-hand relationships would not be selected, and the BOLD signal would be low. New control modules more appropriate for these temporal asynchronies would not yet be learned within the brief and randomly presented trials at each condi-

tion. Thus, as demonstrated, the cerebellum would be relatively inactive.

In conclusion, previous imaging studies using parametric variations of movement parameters (amplitude⁴¹, rate^{42,43}, velocity¹⁹, difficulty⁴⁴) have shown responses distributed throughout the motor system. Our study has exposed activity constrained to the cerebellum and is thus powerful support for its role, suggested from physiology and theory, in the coordination of eye and hand movements.

METHODS

Subjects. Nine right-handed subjects (4 male, 5 female, 21–55 years old) performed two tracking experiments in a single scanning session, after pre-training in the laboratory. Another group of seven (3 female, 18–21 years old) performed experiment 3. Three of the original 9 subjects performed experiment 4, one year after the first two. Subjects gave signed informed consent, and experiments were approved by the Central Oxford Research Ethics Committee.

Tracking protocol. Subjects lay supine in the MR magnet and used prismatic glasses to view a rear projection screen placed 2.8 m from their eyes. The $13^\circ \times 10^\circ$ display was generated by a PC computer, projecting at VGA resolution (640×480) with an LCD projector. Vision was uncorrected but all subjects could see the screen display without difficulty. Subjects held a lightweight, custom-made joystick in their right hands; movement of each joystick in two dimensions was encoded by rotation of polarized disks, detected by fiber optics, converted to voltage signals and sampled at 26 Hz. A square green cursor ($0.2^\circ \times 0.2^\circ$) was controlled by the joystick; subjects were instructed to center this cursor on a large stationary cross hair. In manual tracking conditions—that is, using the hand-held joystick—the cursor was actively displaced from the cross hair following a target waveform, and the task was to compensate for this motion ('compensatory tracking'⁴⁵). Movement of the tip of the joystick of approximately 6 cm (75° of joystick motion) was required, using thumb, finger and wrist movements.

The target for all ocular tracking movements was a white circle, 0.2° in diameter. Eye movement was not recorded in the MR environment but was recorded monocularly in six subjects performing experiments 1 and 2 using an ASL 501 two-dimensional infrared reflectometry eyetracker outside the scanner (R.C.M. & G.Z.R., unpublished data). Accurate tracking of the ocular target required eye movement of up to 10° horizontally, 7.5° vertically and maximum speeds of approximately 6° per second.

Manual tracking performance was quantified by calculating RMS error between the cursor position and the cross hairs, and by cross correlation of joystick and manual target trajectories. RMS error varied from trial to trial because of the difference in mean target speed (randomized target trajectories); hence, all RMS errors were normalized by mean target speed per trial²². Peak cross-correlation coefficients were high (mean r^2 per subject per condition > 0.98) and thus an insensitive performance measure; only correlation lag and normalized RMS errors are reported.

Imaging. Echo-planar imaging (TE, 30 ms; flip angle, 90 degrees) was done with a 3 T Siemens-Varian scanner, with whole brain images in the axial plane. Field of view was 256×256 mm (64×64 voxels), and 21 slices (7 mm) were acquired at a TR of 3 s. For experiment 1, 212 volumes were acquired (10 min 22 s); 290 volumes were acquired for experiment 2 (14 min 30 s). Finally, a T1-weighted structural image was taken, $256 \times 256 \times 21$ voxels. For experiments 3 and 4, 426 or 402 volumes were acquired (21.5 or 20 min) with 25 slices of 5.5 mm at a TR of 3 s.

Image analysis. EPI images were motion corrected to the tenth volume of each series using AIR⁴⁶. They were then spatially filtered, and transformed to a common space by registration of the EPI image to the structural image with a 6° freedom linear transform and of the structural image to the MNI-305 average brain with a 12° freedom affine transform.



Analysis was carried out using FEAT, the FMRIB FSL extension of MEDx (Sensor Systems, Sterling, Virginia). Data were analyzed using general linear modeling within the FSL libraries with local autocorrelation correction. Statistical parametric maps were combined across subjects with fixed-effect models; random-effect modeling was used for experiment two. Regions of significant activation in the group Z (Gaussianized T) statistic images were found by thresholding at $Z = 2.3$ and then detecting significant clusters based on Gaussian field theory at a probability level of $p < 0.01$ (ref. 47). Significant clusters were rendered as color images onto the MNI-305 standard image. Locations of cluster maxima and local maxima are reported; identification of maxima was examined in the median images of the subjects' brains by reference to published atlases^{48,49}.

Experiment 1: factorial design. Subjects performed 5 tracking conditions, presented 6 times each in blocks of 18 s. A rest or fixation condition was presented every fifth block, when the circular and square icons turned red and remained stationary. The other 4 conditions were pseudorandomly ordered (Fig. 1b–e). These conditions were as follows: ocular tracking, in which only the white circle moved and was tracked by the eyes; manual tracking with compensatory joystick control of the green cursor while maintaining ocular fixation on the stationary white circle; coordinated eye and hand tracking, in which both circle and square moved, requiring simultaneous ocular tracking and compensatory joystick control; and independent eye and hand tracking. In the latter, the target motion of the circle and square was unrelated (Fig. 1e). The ocular and manual target waveforms were the sum of 6 sinusoids (3 for vertical motion, 3 for horizontal) of non-harmonic frequencies (0.233, 0.3 and 1.0 Hz) to give a smooth, unpredictable, 2-dimensional trajectory, and with a new trajectory generated every 18 s trial by randomization of sinusoid phases. Trajectories were attenuated with a half-cosine function over the first and last 3 s of each trial to start and end smoothly at screen center. In coordinated tracking, the eye and hand targets were also randomized in each trial, but were identical, inverted versions of each other. Thus during accurate compensatory tracking, the subject's eye and hand would actually follow identical, simultaneous trajectories (Fig. 1d).

Two general linear models were applied. First, the four active tracking conditions were modeled independently to contrast each against rest, and to contrast coordinated versus independent tracking. Average speed of the joystick measured every 3 s was used as a covariate of no interest because the randomization of the target motion every 18 s trial introduced speed variations between trials^{19,22}. Second, a factorial analysis was performed. Factors were as follows: all hand tracking (hand only and coordinated); all eye tracking (eye only and coordinated); neither (rest/fixation); or both (coordinated). The independent tracking condition and average joystick speed were covariates of no interest.

Experiment 2: parametric design. This experiment immediately followed experiment 1. Six conditions were presented 6 times each, in blocks of 18 s. Every sixth block was rest (fixation), the other five conditions were presented in pseudorandom order, and they were all variants of the coordinated eye and hand condition of experiment 1. Here, temporal asynchrony was introduced between motion of the two targets (Fig. 1f). Thus, the white ocular target followed the same spatial path as the required path of the joystick, leading or lagging its motion by 0, 152 or 304 ms. The synchronous (0 ms offset) condition was identical to the coordinated task of experiment 1.

Five levels of eye–hand target asynchrony were modeled as separate factors in a general linear model fit, allowing activation that co-varied with temporal offsets to be detected. Average speed of joystick motion was included as a covariate of no interest. Regions of activation quadratically related to the temporal offset between the two target functions were identified using contrast weights of [+2, -1, -2, -1, +2] or [-2, +1, +2, +1, -2], respectively.

Experiment 3: combined design A. Subjects performed 7 conditions presented 10 times each, again in blocks of 18 s duration. Every seventh block was rest (fixation) as before. The other 6 conditions were presented in pseudorandom order with temporal offset conditions of +304,

+152, 0, -152 or -304 ms, and with independent eye–hand tracking.

The six active conditions were modeled as separate factors, with joystick speed a covariate of no interest. Activation areas were identified using the regression weights of [-5, +1, +3, +1, -5, +5].

Experiment 4: combined design B. Six conditions were presented 11 times each, again in blocks of 18 s duration. Every sixth block was rest (fixation); the other five conditions were presented in pseudorandom order with temporal offset conditions of 0, -152, -304 or -456 ms and independent eye–hand tracking (same as experiment 1).

The five active conditions were modeled as separate factors, with joystick speed a covariate of no interest. Activation areas were identified using the quadratic regression weights of [+2, -1, -2, -1, +2], or by contrasts of [+1, 0, -1, 0, 0] and [0, 0, -1, 0, +1].

All subjects were trained, and practiced the tasks in the laboratory one or two days before scanning, using a similar joystick and display. They also practiced for 5–15 minutes in the scanner during preliminary localizing scans and shimming.

ACKNOWLEDGEMENTS

We thank the Wellcome Trust, JST ERATO, the Oxford FMRIB and MRC Cognitive Neuroscience Centers for help and facilities, and G. Swait and N. Jenkinson for supplementary data collection.

RECEIVED 15 MARCH; ACCEPTED 9 APRIL 2001

- Flourens, P. *The Human Brain and Spinal Cord* (eds. Clarke, E. & O'Malley, C. D.) 657–661 (Univ. California Press, Berkeley, 1968).
- Bastian, A. J., Martin, T. A., Keating, J. G. & Thach, W. T. Cerebellar ataxia: abnormal control of interaction torques across multiple joints. *J. Neurophysiol.* **76**, 492–509 (1996).
- Muller, F. & Dichgans, J. Dyscoordination of pinch and lift forces during grasp in patients with cerebellar lesions. *Exp. Brain Res.* **101**, 485–492 (1994).
- Serrien, D. J. & Wiesendanger, M. Temporal control of a bimanual task in patients with cerebellar dysfunction. *Neuropsychologia* **38**, 558–565 (2000).
- Van Donkelaar, P. & Lee, R. G. Interactions between the eye and hand motor systems: disruptions due to cerebellar dysfunction. *J. Neurophysiol.* **72**, 1674–1685 (1994).
- Vercher, J. L. & Gauthier, G. M. Cerebellar involvement in the coordination control of the oculo-manual tracking system: effects of cerebellar dentate nucleus lesion. *Exp. Brain Res.* **73**, 155–166 (1988).
- Miall, R. C. The cerebellum, predictive control and motor coordination. *Novartis Found. Symp.* **218**, 272–290 (1998).
- Miall, R. C., Imamizu, H. & Miyauchi, S. Activation of the cerebellum in coordinated eye and hand tracking movements: an fMRI study. *Exp. Brain Res.* **135**, 22–33 (2000).
- Marple-Horvat, D. E., Criado, J. M. & Armstrong, D. M. Neuronal activity in the lateral cerebellum of the cat related to visual stimuli at rest, visually guided step modification, and saccadic eye movements. *J. Physiol. (Lond.)* **506**, 489–514 (1998).
- Abrams, R. A., Meyer, D. E. & Kornblum, S. Eye–hand coordination: oculomotor control in rapid aimed limb movements. *J. Exp. Psychol.* **16**, 248–267 (1990).
- Koken, P. W. & Erkelens, C. J. Influences of hand movements on eye movements in tracking tasks in man. *Exp. Brain Res.* **88**, 657–664 (1992).
- Vercher, J. L., Mageses, G., Prablanc, C. & Gauthier, G. M. Eye–head–hand coordination in pointing at visual targets: spatial and temporal analysis. *Exp. Brain Res.* **99**, 507–523 (1994).
- Biguer, B., Prablanc, C. & Jeannerod, M. The contribution of coordinated eye and head movements in hand pointing accuracy. *Exp. Brain Res.* **55**, 462–469 (1984).
- Petit, L. & Haxby, J. V. Functional anatomy of pursuit eye movements in humans as revealed by fMRI. *J. Neurophysiol.* **82**, 463–471 (1999).
- Berman, R. A. *et al.* Cortical networks subserving pursuit and saccadic eye movements in humans: an fMRI study. *Hum. Brain Mapp.* **8**, 209–225 (1999).
- Nishitani, N. Cortical visuomotor integration during eye pursuit and eye–finger pursuit. *J. Neurosci.* **19**, 2647–2657 (1999).
- Grafton, S. T., Mazziotta, J. C., Woods, R. P. & Phelps, M. E. Human functional anatomy of visually guided finger movements. *Brain* **115**, 565–587 (1992).
- Jueptner, M., Jenkins, I. H., Brooks, D. J., Frackowiak, R. S. J. & Passingham, R. E. The sensory guidance of movement: a comparison of the cerebellum and basal ganglia. *Exp. Brain Res.* **112**, 462–474 (1996).
- Turner, R. S., Grafton, S. T., Votaw, J. R., DeLong, M. R. & Hoffman, J. M. Motor subcircuits mediating the control of movement velocity: a PET study. *J. Neurophysiol.* **80**, 2162–2176 (1998).



20. Jenkins, I. H., Brooks, D. J., Nixon, P. D., Frackowiak, R. S. J. & Passingham, R. E. Motor sequence learning: a study with positron emission tomography. *J. Neurosci.* **14**, 3775–3790 (1994).
21. Clower, D. M. *et al.* Role of posterior parietal cortex in the recalibration of visually guided reaching. *Nature* **383**, 618–621 (1996).
22. Imamizu, H. *et al.* Human cerebellar activity reflecting an acquired internal model of a new tool. *Nature* **403**, 192–195 (2000).
23. Flament, D., Ellermann, J. M., Kim, S. G., Ugurbil, K. & Ebner, T. J. Functional magnetic resonance imaging of cerebellar activation during the learning of a visuomotor dissociation task. *Hum. Brain Mapp.* **4**, 210–226 (1996).
24. Allen, G., Buxton, R. B., Wong, E. C., Courchesne, E. Attentional activation of the cerebellum independent of motor involvement. *Science* **275**, 1940–1943 (1997).
25. Ivry, R. Cerebellar timing systems. *Int. Rev. Neurobiol.* **41**, 555–573 (1997).
26. Shadmehr, R. & Holcomb, H. H. Neural correlates of motor memory consolidation. *Science* **277**, 821–825 (1997).
27. Roland, P. E. & Gulyas, B. Visual memory, visual imagery, and visual recognition of large field patterns by the human brain: functional anatomy by positron emission tomography. *Cereb. Cortex* **5**, 79–93 (1995).
28. Fletcher, P. C., Shallice, T., Frith, C. D., Frackowiak, R. S. & Dolan, R. J. Brain activity during memory retrieval. The influence of imagery and semantic cueing. *Brain* **119**, 1587–1596 (1996).
29. Ghaem, O. *et al.* Mental navigation along memorized routes activates the hippocampus, precuneus, and insula. *Neuroreport* **8**, 739–744 (1997).
30. Tamada, T., Miyauchi, S., Imamizu, H., Yoshioka, T. & Kawato, M. Cerebro-cerebellar functional connectivity revealed by the laterality index in tool-use learning. *Neuroreport* **10**, 325–331 (1999).
31. Van Donkelaar, P., Lee, R. G. & Gellman, R. S. The contribution of retinal and extraretinal signals to manual tracking movements. *Exp. Brain Res.* **99**, 155–163 (1994).
32. Ferraina, S. *et al.* Visual control of hand-reaching movement: activity in parietal area 7m. *Eur. J. Neurosci.* **9**, 1090–1095 (1997).
33. Vercher, J. L. *et al.* Self-moved target eye tracking in control and deafferented subjects: roles of arm motor command and proprioception in arm-eye coordination. *J. Neurophysiol.* **76**, 1133–1144 (1996).
34. Witney, A. G., Goodbody, S. J. & Wolpert, D. M. Predictive motor learning of temporal delays. *J. Neurophysiol.* **82**, 2039–2048 (1999).
35. Miall, R. C. & Wolpert, D. M. Forward models for physiological motor control. *Neural Net.* **9**, 1265–1279 (1996).
36. Pelisson, D., Prablanc, C., Goodale, M. A. & Jeannerod, M. Visual control of reaching movements without vision of the limb. II. Evidence of fast unconscious processes correcting the trajectory of the hand to the final position of a double-step stimulus. *Exp. Brain Res.* **62**, 303–311 (1986).
37. Lewis, R. F., Gaymard, B. M. & Tamargo, R. J. Efference copy provides the eye position information required for visually guided reaching. *J. Neurophysiol.* **80**, 1605–1608 (1998).
38. Miall, R. C., Weir, D. J. & Stein, J. F. Visuomotor tracking with delayed visual feedback. *Neuroscience* **16**, 511–520 (1985).
39. Vercher, J. L. & Gauthier, G. M. Oculo-manual coordination control: ocular and manual tracking of visual targets with delayed visual feedback of the hand motion. *Exp. Brain Res.* **90**, 599–609 (1992).
40. Wolpert, D. M. Multiple paired forward and inverse models for motor control. *Neural Net.* **11**, 1317–1329 (1998).
41. Waldvogel, D., van Gelderen, P., Ishii, K. & Hallett, M. The effect of movement amplitude on activation in functional magnetic resonance imaging studies. *J. Cereb. Blood Flow Metab.* **19**, 1209–1212 (1999).
42. Vanmeter, J. W. *et al.* Parametric analysis of functional neuroimages—application to a variable-rate motor task. *Neuroimage* **2**, 273–283 (1995).
43. Jenkins, I. H., Passingham, R. E. & Brooks, D. J. The effect of movement frequency on cerebral activation: a positron emission tomography study. *J. Neurol. Sci.* **151**, 195–205 (1997).
44. Winstein, C. J., Grafton, S. T. & Pohl, P. S. Motor task difficulty and brain activity: Investigation of goal-directed reciprocal aiming using positron emission tomography. *J. Neurophysiol.* **77**, 1581–1594 (1997).
45. Poulton, E. C. *Tracking Skill and Manual Control* (Academic, New York, 1974).
46. Woods, R. P., Grafton, S. T., Holmes, C. J., Cherry, S. R. & Mazziota, J. C. Automated image registration: I. General methods and intrasubject, intramodality validation. *J. Comput. Assist. Tomogr.* **22**, 141–154 (1998).
47. Friston, K. J., Worsley, K. J., Frackowiak, R. S. J., Mazziota, J. C. & Evans, A. C. Assessing the significance of focal activations using their spatial extent. *Hum. Brain Mapp.* **1**, 214–220 (1994).
48. Talairach, J. & Tournoux, P. *Co-Planar Stereotaxic Atlas of the Human Brain* (Thieme, Stuttgart, 1988).
49. Schmahmann, J. D. *et al.* Three-dimensional MRI atlas of the human cerebellum in proportional stereotaxic space. *Neuroimage* **10**, 233–260 (1999).